Electron-Excitation–Gamma-Decay Reactions in Heavy Nuclei*

T. A. Griffy and Don Whitehill
Department of Physics, The University of Texas, Austin, Texas 78712
(Received 8 May 1970)

The feasibility of using the reactions

$$e+N(\epsilon_i, J_i) \rightarrow e'+N(\epsilon_f, J_f)$$
$$\searrow N(\epsilon_{ff}, J_{ff})+\gamma$$

to investigate low-lying states of heavy nuclei is discussed. By detecting the decay photon, the problem of poor energy resolution for high-energy electrons can be circumvented. The formalism for the e'-γ coincidence cross section is given. The Coulomb distortion of the electron wave functions, which is important for heavy nuclei, is taken into account. Results for the e'-γ coincidence cross section and the γ-detection cross section for several nuclei are given. The e-γ coincidence cross section appears to be feasible when superconducting accelerators became operational. The γ-detection cross section offers a method for investigating low-lying states with present-day accelerators.

I. INTRODUCTION

With the rapid advance in the design of high-energy electron accelerators, electrons have proved to be quite useful probes for investigating nuclear structure.[1,2] Most theoretical investigations of electron scattering from nuclei have involved detection of only the final electron. Additional nuclear-structure information can be obtained by detecting other final particles from reactions initiated by electron scattering. Coincidence detection of two or more final-state particles would be particularly advantageous for studying specific aspects of nuclear structure, but electron scattering cross sections are so small that coincidence detection experiments are often impossible to perform. However, the development of high-intensity high-duty-cycle accelerators, especially superconducting accelerators,[3] is opening new areas of experimental investigation and theoretical interest in electron-nucleus scattering.

The reaction considered here is electron excitation of a nucleus with subsequent decay of the excited state,

$$e+N(\epsilon_i, J_i M_i) \rightarrow e'+N(\epsilon_f, J_f M_f)$$
$$\searrow \gamma+N(\epsilon_{ff}, J_{ff} M_{ff}). \tag{1.1}$$

Here $N(\epsilon, JM)$ denotes a nucleus with energy ϵ, spin J, and spin projection on the z-axis M (Fig. 1). For the electron energies required, on the order of a 100 MeV, the energy resolution for the electrons precludes investigations of nuclear states with excitation energies less than a few MeV when only the final electron is detected. Detection of the decay photon enables investigation of low-lying states such as occur in heavy nuclei, since the energy resolution for the photon is much better than for the electron. For photon energies of a few hundred keV, the energy resolution is on the order of a keV. The e'-γ coincidence cross section is derived in Sec. II, and results for the e'-γ coincidence cross section and for the γ-detection cross section are given in Sec. III.

The e'-γ coincidence cross section has previously been studied with the derivation based on the first-order Born approximation.[4,5,6] The validity of using the first-order Born approximation depends on being able to neglect all terms proportional to $(Z\alpha)^2$ and of higher order in a perturbation expansion. As Z becomes large the results of Born-approximation calculations become questionable. It has previously been shown that it may be necessary to use the method of Coulomb-distorted plane waves when scattering electrons from heavy nuclei.[7] This method takes into account the effect of the static Coulomb field of the nucleus in the electron wave functions. All derivations and results given here employ the method of Coulomb-distorted plane waves for high-energy electrons.

Since the purpose of this study is primarily to determine the feasibility of using the reactions in Eq. (1.1) to investigate low-lying excited states of heavy nuclei, a few simplifying assumptions are made. Both the excitation and deexcitation processes are assumed to have only one contributing multipole moment. This is a good approximation when the lowest allowed multipole moment is electric, especially for the excitation process. In this case the electron excitation term is dominated by the Coulomb part of the interaction. When the lowest

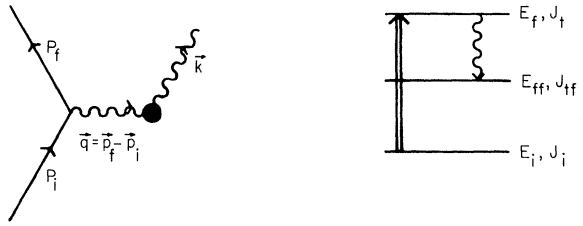

FIG. 1. Diagram and nuclear energy levels for the reaction

$$e+N(\epsilon_i, J_i) \rightarrow e'+N(\epsilon_f, J_f)$$
$$\searrow N(\epsilon_{ff}, J_{ff})+\gamma.$$

multipole moment is magnetic, mixed multipole transitions are likely to occur. The recoil of the nucleus is neglected, since only heavy nuclei are to be considered. Coherent interference from other processes is also ignored. Two main sources of interference are elastic electron scattering plus production of electron bremsstrahlung and electron excitation of more energetic nuclear states followed by cascade decays through the excited state to be investigated. Since bremsstrahlung is strongly forward peaked for high-energy electrons, its interference can be minimized by looking for the decay photons at large angles to the incident and scattered electron directions. Only excitations of higher-energy states lying within the energy resolutions for the electron of the state to be investigated can lead to interfering cascade decays. The cascade decay through the excited state of interest is of higher order in α than the reaction in Eq. (1.1). Therefore, it is expected to have a smaller amplitude.

II. DERIVATION OF CROSS SECTION

A. Electron Excitation

Here we are interested in the electron-excitation part of the two-step reaction in Eq. (1.1). We work in the lab frame of the nucleus for the incident beam in the $+z$ direction and the momentum of the scattered electron is $\vec{p}_f$. The electron wave functions are distorted plane waves in the presence of the static Coulomb field of the nucleus (see Appendix).

Under the assumption that only one multipole contributes to the excitation, the spatial part of the nuclear transition charge and current can be written as ($\hbar = c = 1$).

$$\langle \Phi(\epsilon_f, J_f M_f)|j^0(\vec{r})|\Phi(\epsilon_i, J_i M_i)\rangle = e\sum_\mu C^{J_i\ \lambda\ J_f}_{M_i\ \mu\ M_f}\rho_\lambda(r)Y^{\mu *}_\lambda(\hat{r}), \tag{2.1}$$

$$\langle \Phi(\epsilon_f, J_f M_f)|\vec{j}(r)|\Phi(\epsilon_i, J_i M_i)\rangle = e\sum_\mu C^{J_i\ \lambda\ J_f}_{M_i\ \mu\ M_f}[\rho_{\lambda,\lambda+1}(r)\vec{Y}^{\mu *}_{\lambda,\lambda+1}(\hat{r})+\rho_{\lambda,\lambda-1}(r)\vec{Y}^{\mu *}_{\lambda,\lambda-1}(\hat{r})+\rho_{\lambda,\lambda}(r)\vec{Y}^{\mu}_{\lambda,\lambda}(\hat{r})].$$

In the above, $\Phi(\epsilon, JM)$ denotes the wave functions for the nucleus in the state with the quantum numbers as specified in the brackets. The nuclear transition charge and current operators are $j^0(\vec{r})$ and $\vec{j}(\vec{r})$.

Using first-order time-dependent perturbation, the transition amplitude for electron excitation of the nucleus can be written as

$$S_{i\rightarrow f} = 2\pi i\delta(E_f - E_i + \epsilon_f - \epsilon_i)\int d^3r\,\langle \Phi(\epsilon_f, J_f M_f)|j^\mu(\vec{r})|\Phi(\epsilon_i, J_i M_i)\rangle A_\mu(\vec{r}). \tag{2.2}$$

$A^\mu(\vec{r})$ is the electromagnetic four-vector potential due to the electron transition current, and E_f and E_i are initial and final electron energies. Upon expanding the electron wave function in partial waves, the transition amplitude for initial electron spin m and final spin m' can be put in the form

$$S_{i\rightarrow f}(M_i, m; M_f, m') = 2\pi\delta(E_f - E_i + \epsilon_f - \epsilon_i)\sum_\mu C^{J_i\ \lambda\ J_f}_{M_i\ \mu\ M_f}(-)^\mu S_{\lambda,-\mu}(m, m'), \tag{2.3}$$

where

$$S_{\lambda\mu}(m, m') = 8\pi^2\alpha\omega\left[\frac{(E_i+m_e)(E_f+m_e)}{E_i E_f V^2}\right]^{1/2}\sum_{\kappa\kappa'}\{e^{i(\bar{\delta}'_{\kappa'}+\bar{\delta}_\kappa)}\, i^{l-l'}(-)^{j'+l+\lambda+1/2}(2l+1)[(2\lambda+1)(2j+1)]^{1/2}$$
$$\times C^{l\ 1/2\ j}_{0\ m\ m}\, C^{l'\ 1/2\ j'}_{m+\mu-m'\ m'\ m+\mu}\, C^{j\ \lambda\ j'}_{m\ \mu\ m+\mu}\, Y^{m-\mu-m'}_{l'}(\hat{p}_f)[C^{l\ \lambda\ l'}_{0\ 0\ 0}\, W(j'l'jl;\tfrac{1}{2}\lambda)R^E(\kappa\lambda\kappa')$$
$$+ C^{l\ \lambda\ \bar{l}'}_{0\ 0\ 0}\, W(j'\bar{l}'jl;\tfrac{1}{2}\lambda)R^M(\kappa\lambda\kappa')]\}. \tag{2.4}$$

The primed quantities refer to the final electron, and the unprimed quantities refer to the initial electron. The relation of l and j to k is given in the Appendix, and $\bar{l}' = l' - \kappa'/|\kappa'|$. The radial integrals are given by ($\omega = E_i - E_f$)

$$R^E(\kappa\lambda\kappa') = \int_0^\infty dr_1 \int_0^\infty dr_2 r_1^2 r_2^2 \Big(j_\lambda(\omega r_<) h_\lambda^{(1)}(\omega r_>) \rho_\lambda(r_1) [g'_{\kappa'}(r_2) g_\kappa(r_2) + f'_{\kappa'}(r_2) f_\kappa(r_2)]$$
$$+ i[\lambda(\lambda+1)]^{-1/2} j_{\lambda-1}(\omega r_<) h_{\lambda-1}^{(1)}(\omega r_>) \rho_{\lambda,\lambda-1}(r_1) \{\lambda[g'_{\kappa'}(r_2) f_\kappa(r_2) - f'_{\kappa'}(r_2) g_\kappa(r_2)]$$
$$+ (\kappa - \kappa')[g'_{\kappa'}(r_2) f_\kappa(r_2) + f'_{\kappa'}(r_2) g_\kappa(r_2)]\} - i[(\lambda+1)(\lambda+2)]^{-1/2} j_{\lambda+1}(\omega r_<) h_{\lambda-1}^{(1)}(\omega r_>) \rho_{\lambda,\lambda+1}(r_1)$$
$$\times \{(\lambda+1)[g'_{\kappa'}(r_2) f_\kappa(r_2) - f'_{\kappa'}(r_2) g_\kappa(r_2)] - (\kappa - \kappa')[g'_{\kappa'}(r_2) f_\kappa(r_2) + f'_{\kappa'}(r_2) g_\kappa(r_2)]\}\Big), \tag{2.5a}$$

$$R^M(\kappa\lambda\kappa') = \int_0^\infty dr_1 \int_0^\infty dr_2 r_1^2 r_2^2 j_\lambda(\omega r_<) h_\lambda^{(1)}(\omega r_>) \rho_{\lambda,\lambda}(r_1) i[\lambda(\lambda+1)]^{-1/2} (\kappa + \kappa')[g'_{\kappa'}(r_2) f_\kappa(r_2) + f'_{\kappa'}(r_2) g_\kappa(r_2)] . \tag{2.5b}$$

The functions $f_\kappa(r)$ and $g_\kappa(r)$ are the radial parts of the electron wave functions.

The differential electron excitation cross section for an unpolarized electron beam incident on an unpolarized target and with final polarization not detected is

$$\frac{d\sigma_{\rm IN}}{d\Omega_e} = \tfrac{1}{2} \frac{E_i E_f p_f}{(2\pi)^2 p_i} V^2 \frac{1}{2J_i+1} \sum_{\substack{m m' \\ M_i M_f}} \Big| \sum_\mu C^{J_i \; \lambda \; J_f}_{M_i \; \mu \; M_f} (-)^\mu S_{\lambda-\mu}(m, m') \Big|^2 . \tag{2.6}$$

B. e'-γ Angular Correlation and Cross Section

The angular correlation between the direction of the scattered electron and decay photon is given by

$$W_{\vec q}(\Omega_\gamma) = \sum_{\sigma M_i M_{ff}} \Big| \sum_{M_f} \langle \Phi(\epsilon_{ff}, J_{ff} M_{ff}) | H_\gamma(\Omega_\gamma, \sigma) | \Phi(\epsilon_f, J_f M_f) \rangle \langle \Phi(\epsilon_f, J_f M_f) | H_{\rm el}(\vec q) | \Phi(\epsilon_i, J_i M_i) \rangle \Big|^2 . \tag{2.7}$$

$H(\Omega_\gamma, \sigma)$ is the interaction Hamiltonian for emission of a photon with polarization σ into the solid angle Ω_γ. $H_{\rm el}(\vec q)$ is the interaction Hamiltonian for electron excitation of the nucleus with electron three-momentum transfer $\vec q$ as developed in part A of this Section.

After making a multipole expansion of the interaction Hamiltonians and carrying out the appropriate sums, $W_{\vec q}(\Omega_\gamma)$ takes the form[8,9]

$$W_{\vec q}(\Omega_\gamma) = N \sum_{\substack{\text{even} \\ \kappa}} \sum_k [-1/(2k+1)^{1/2}] \begin{pmatrix} \lambda & \lambda & k \\ 1 & -1 & 0 \end{pmatrix}^{-1} \sum_{\mu\mu'} (-)^{\mu+\kappa} \begin{pmatrix} \lambda & \lambda & k \\ \mu & -\mu' & \kappa \end{pmatrix} \sum_{\mu\mu'} S_{\lambda\mu}(m, m') S_{\lambda\mu}^*(m, m')$$
$$\times F_k(\lambda\lambda J_i J_f) \sum_{LL'} (-)^{L+L'} F_k(L L' J_{ff} J_f) A_L^M A_{L'}^{M'} Y_k^\kappa(\Omega_\gamma) . \tag{2.8}$$

A_L^M is the reduced matrix element for the ML multipole moment and is real for the appropriate choice of phase convention for the nuclear states.[10] N is a normalization factor chosen such that

$$\int W_{\vec q}(\Omega_\gamma) d\Omega_\gamma = 1 . \tag{2.9}$$

It is assumed that only one multipole contributes to the γ-decay transition for the results given in this paper. In the case of an L-pole decay following a λ-pole electron excitation $A_{L'}^{M'} = \delta_{LL'} \delta_{MM'} A_L^M$ and

$$N = \Big[\sqrt{4\pi}\, F_0(\lambda\lambda J_i J_f) F_0(LL J_{ff} J_f)$$
$$\times (A_L^M)^2 \sum_{\mu m m'} |S_{\lambda\mu}(m, m')|^2 \Big]^{-1} .$$

The e-γ coincidence cross section can now be written as

$$\frac{d^2\sigma}{d\Omega_e d\Omega_\gamma} = \frac{d\sigma_{\rm IN}}{d\Omega_e} W_{\vec q}(\Omega_\gamma) \frac{\Gamma_\gamma}{\Gamma_{\rm tot}} . \tag{2.10}$$

Γ_γ is the partial decay width for the γ decay of $N(\epsilon_f, J_t)$ to $N(\epsilon_{ff}, J_{ff})$. $\Gamma_{\rm tot}$ is the total decay width for the state $N(\epsilon_f, J_t)$.

III. CALCULATIONS

The formalism for the $(e, e'\gamma)$ reaction presented in Sec. II is independent of the nuclear model except for the assumption of a spherically symmetric static charge distribution for the nucleus. The quantized liquid-drop model for the nucleus is used for all calculations reported here. This model relates the nuclear transition charge and current distributions to the static nuclear charge distribution. The static charge distribution is assumed to be a Fermi distribution given by

$$\rho_0(r) = \{1 + \exp[(r - c/t)4.4]\}^{-1} , \tag{3.1}$$

where the nuclear half radius is given in terms of the number of nucleons A by $c = 1.07 \times A^{1/3}$ F, and the skin thickness t is 2.4 F. All electron-excitation transitions considered here are of the type $E\lambda$. For $E\lambda$ transitions, the transition charge and

TABLE I. Summary of transitions investigated and parameters used in the calculations.

Nucleus	$J_i^{\pi} i$, $J_f^{\pi} ff$	E_f (keV)	$J_f^{\pi} f$	$M\lambda$ excit.	ML decay	$\frac{1}{\alpha^2} B(E\lambda; J_i \to J_f)$ (fm^2)	$\frac{\Gamma_\gamma}{\Gamma_{tot}}$
$_{88}Ra^{222}$	$0^+ i$, $0^+ ff$	242	1^-	$E1$	$E1$	7.09[a]	0.928
$_{82}Pb^{206}$	$0^+ i$, $0^+ ff$	810	2^+	$E2$	$E2$	1.4×10^{3}[b]	1.0
$_{82}Pb^{208}$	0^+	2600	3^-	$E3$	$E3$	5.61×10^{5}[c]	1.0
$_{73}Ta^{181}$	$\frac{7}{2}^+$	136	$\frac{9}{2}^+$	$E2$	$M1, E2$	1.9×10^{4}[b]	1.0

[a] Single-particle estimate. [b] See Ref. 8. [c] See Ref. 1.

current distributions occurring in the electron-excitation amplitude are[11]

$$\rho_\lambda(r) = r^{\lambda-1}\,\partial\rho_0(r)/\partial r\,, \tag{3.2a}$$

$$\rho_{\lambda,\lambda-1}(r) = i\omega[(2\lambda+1)/\lambda]^{1/2} r^{\lambda-1}\rho_0(r)\,, \tag{3.2b}$$

$$\rho_{\lambda,\lambda+1}(r) = \rho_{\lambda,\lambda}(r) = 0\,. \tag{3.2c}$$

The relative normalization of $\rho_\lambda(r)$ and $\rho_{\lambda,\lambda-1}(r)$ is chosen to satisfy the continuity equation, but the absolute normalization of the transition charge is factored out of the calculation by dividing out the reduced nuclear transition probability given by

$$\frac{1}{\alpha^2} B(E\lambda; J_i \to J_f) = \frac{2J_f+1}{2J_i+1}\left[\frac{(2\lambda+1)}{\omega^\lambda}\int_0^\infty dr\, r^2 \rho_\lambda(r) j_\lambda(\omega r)\right]^2. \tag{3.3}$$

The e-γ coincidence cross section is calculated for four different nuclei. The table gives the energy and spins of the states involved. In each case the initial state is the ground state, and the excited state decays back to the ground state. The multipolarity of the transition is also given. In the case of $_{73}Ta^{181}$, two multipoles are known to contribute significantly to the decay process. However, the calculation is done assuming a pure $M1$ or pure $E2$ mode. The last two columns in the table give the values used for $B(E\lambda, J_i \to J_f)$ and $\Gamma_\gamma/\Gamma_{tot}$. The value of $\Gamma_\gamma/\Gamma_{tot}$ for $_{88}Ra^{222}$ is obtained assuming the only decay modes to be via γ decay to the 0^+ and 2^+ states and using the ratio $B(E1; \Gamma \to 0^+)/B(E1; 1^- \to 2^+) = 0.5$.[8] The excited states for the other nuclei are assumed to decay only to the ground state via γ

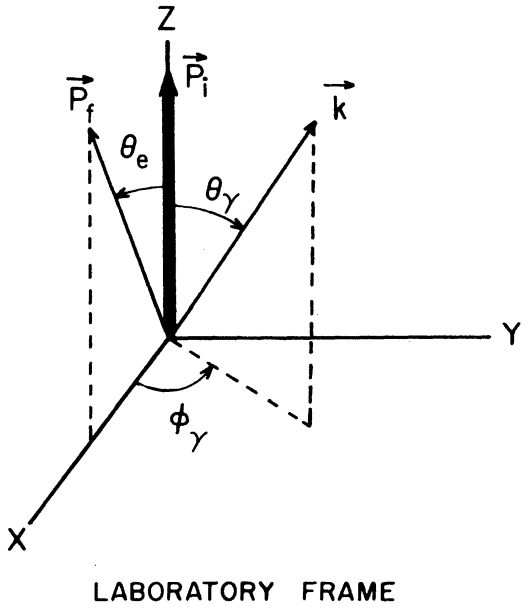

FIG. 2. Lab frame for the nucleus.

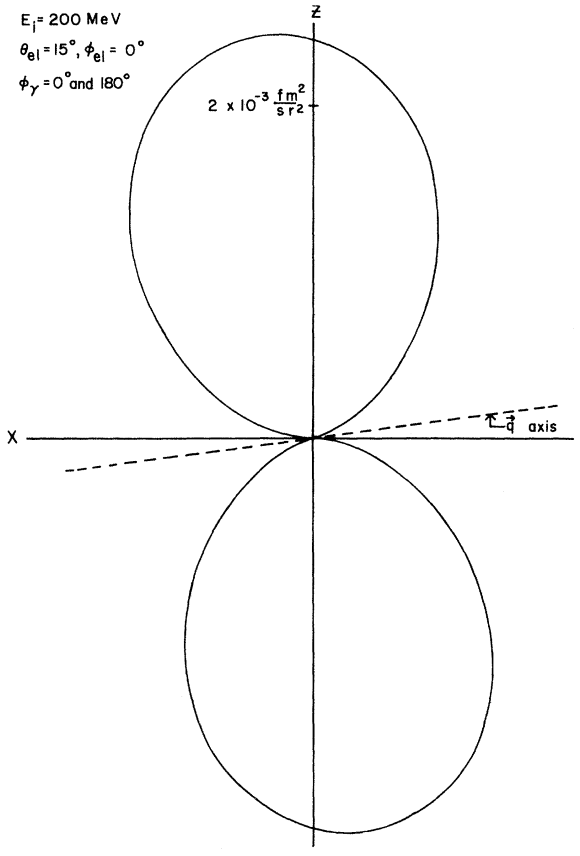

FIG. 3. Polar plot of $d^2\sigma/d\Omega_e d\Omega_\gamma$ versus θ_γ for $_{88}Ra^{222}$.

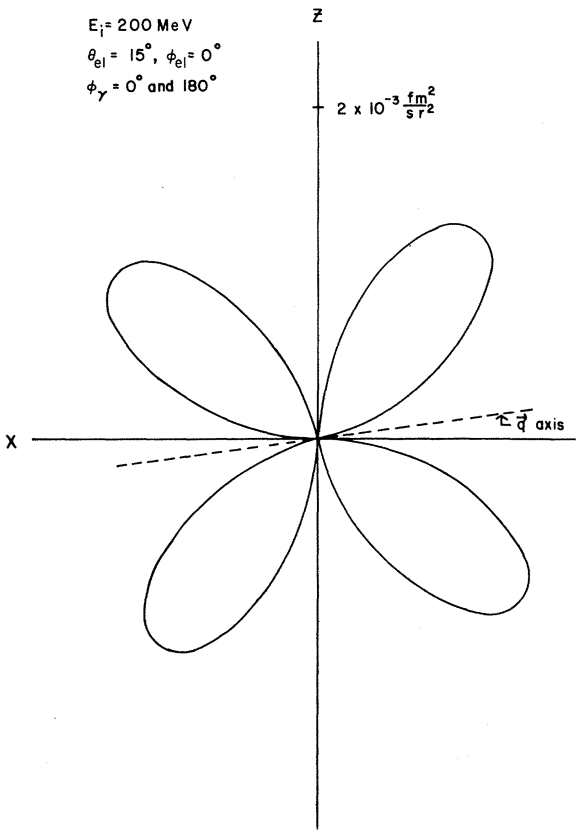

FIG. 4. Polar plot of $d^2\sigma/d\Omega_e d\Omega_\gamma$ versus θ_γ for $_{82}Pb^{206}$.

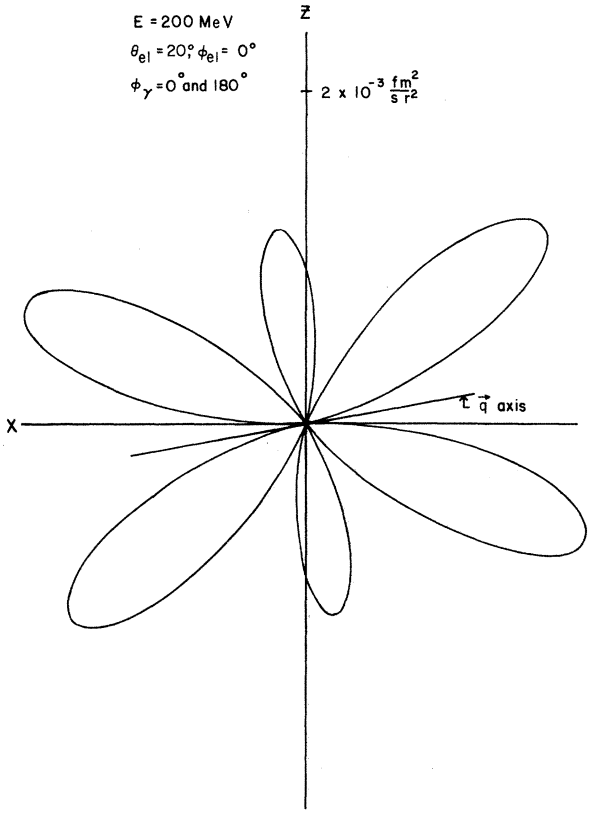

FIG. 5. Polar plot of $d^2\sigma/d\Omega_e d\Omega_\gamma$ versus θ_γ for $_{82}Pb^{208}$.

emission.

All calculations are for the lab frame. The z axis is chosen to be parallel to the incident electron beam momentum $\vec{p}_i$. The x axis is chosen such that $\vec{p}_f$ lies in the x-z plane, and the scalar product $\vec{p}_f \cdot \hat{e}_x$ is positive. The decay-photon momentum is denoted by $\vec{k}$ (see Fig. 2).

Polar plots of the e-γ coincidence cross sections for the nuclei listed in the table are shown in Figs. 3 through 9. In each case the cross section is plotted versus the polar angle θ_γ for photons emitted in the x-z plane. The electron scattering angle θ_e and incident energy E_i are given on each graph. The e-γ coincidence cross section for arbitrary direction of the photon can be obtained by rotating the given plots about the electron-momentum-transfer axis $\vec{q} = \vec{p}_i - \vec{p}_f$. As expected, the polar plots of the e-γ coincidence cross section versus θ_γ for small θ_e have the shapes of L-pole electromagnetic radiation patterns symmetric about the q axis. When using the results of Alder *et al.* in $W_{\vec{q}}(\Omega_\gamma)$ (see Sec. II), the axis of symmetry was reflected through the z axis in the x-z plane.

The cross section for detection of only the decay photon is obtained by integrating over the final-electron direction. Results for the γ-detection cross section for the reaction in the table involving $_{73}Ta^{181}$ are shown in Figs. 10 through 13. The cross sections are plotted versus θ_γ for incident electron energies of 200 and 30 MeV. The cases where the emitted radiation is assumed to be pure $M1$ and pure $E2$ are given.

The information which can be obtained when only the decay photon is detected is not as great as when the scattered electron and decay photon are detected in coincidence. It is not possible to investigate the dependence of the cross section on the electron momentum transfer. In other words, the shapes of the transition charge and current cannot be determined. Also, the γ-radiation pattern is not as sensitive to the multipolarity of the γ decay as is the e-γ correlation. However, the value of the reduced nuclear transition probability $B(E\lambda; J_i \to J_f)$ can be determined.

IV. CONCLUSIONS

The calculations presented in Sec. III are primarily intended to indicate the feasibility of using the $(e, e'\gamma)$ reaction to investigate low-lying states of heavy nuclei. As mentioned before, some simplifying assumptions have been made in the calcula-

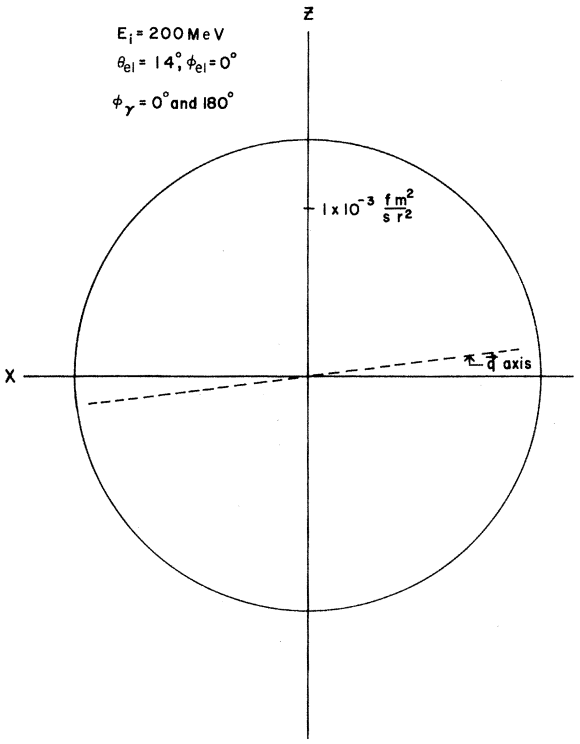

FIG. 6. Polar plot of $d^2\sigma/d\Omega_e d\Omega_\gamma$ versus θ_γ for $_{73}Ta^{181}$ with the decay assumed to be a pure $M1$ transition.

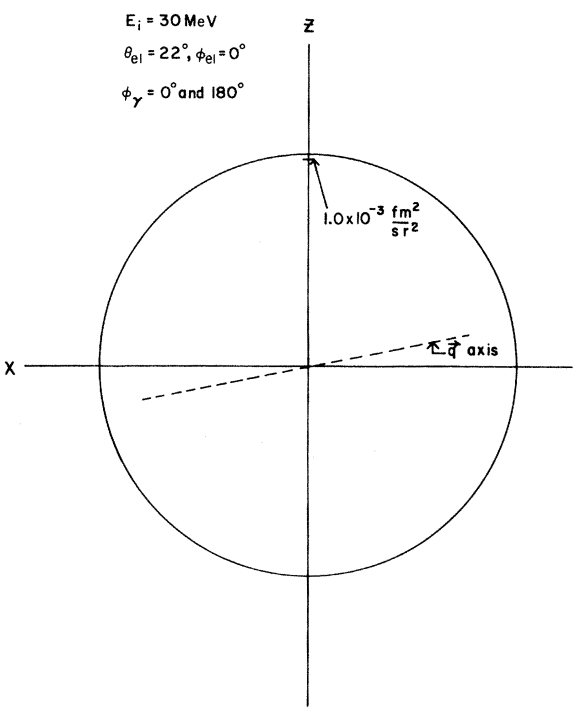

FIG. 8. Polar plot of $d^2\sigma/d\Omega_e d\Omega_\gamma$ versus θ_γ for $_{73}Ta^{181}$ with the decay assumed to be a pure $M1$ transition.

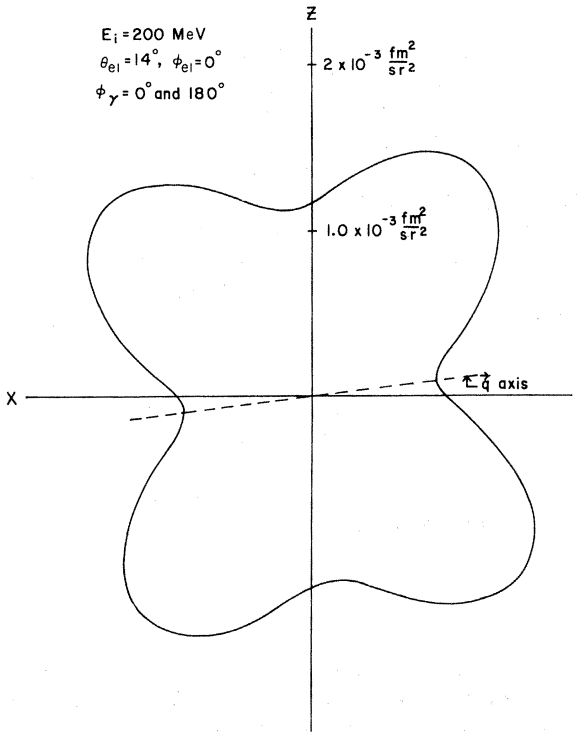

FIG. 7. Polar plot of $d^2\sigma/d\Omega_e d\Omega_\gamma$ versus θ_γ for $_{73}Ta^{181}$ with the decay assumed to be a pure $E2$ transition.

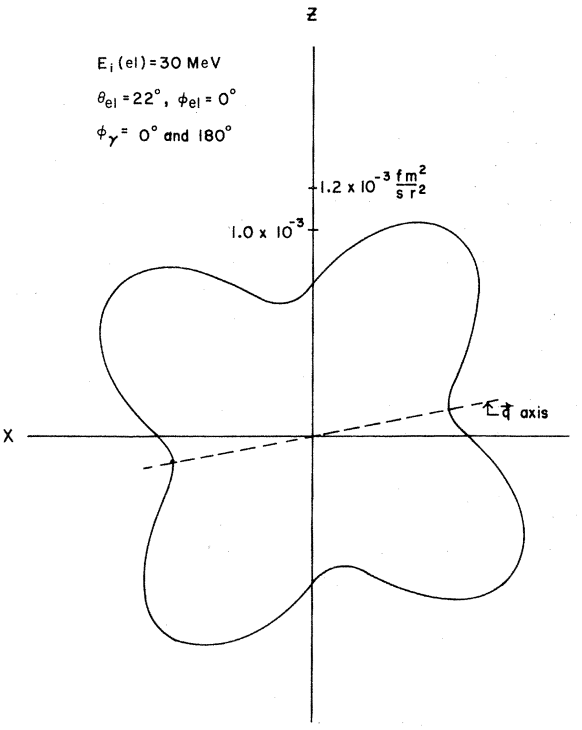

FIG. 9. Polar plot of $d^2\sigma/d\Omega_e d\Omega_\gamma$ versus θ_γ for $_{73}Ta^{181}$ with the decay assumed to be a pure $E2$ transition.

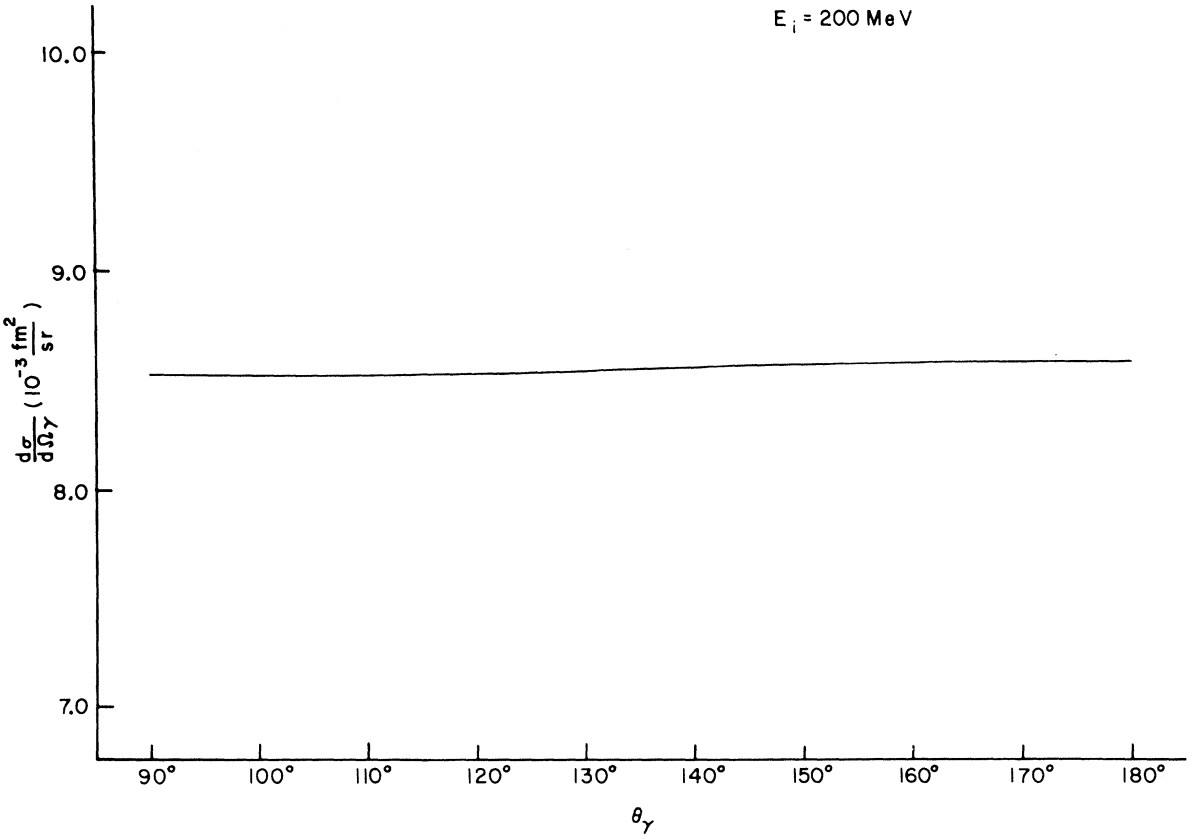

FIG. 10. γ-detection cross section for $_{73}Ta^{181}$ with the decay assumed to be a pure $M1$ transition.

tions. In addition, the nuclear model employed is chosen mostly for convenience, although it is known to give good agreement with electron scattering data. The calculations are unique in that the Coulomb distortion of the electron wave functions, which is important for heavy nuclei, is taken into account. The effects of mixed multipole γ-decay transitions and coherent interference from other processes might have to be included when experimental data becomes available. More sophisticated nuclear models will probably be required also. However, it is premature at this time to worry about specific details leading to minor changes in the results.

The most important information to be obtained from this study is the expected size of the cross section. The cross section must be large enough to yield detectable counting rates and to distinguish the excitation-decay reaction from interfering processes.

The e-γ coincidence counting rate can be estimated from the relation

$$R = \frac{d^2\sigma}{d\Omega_e d\Omega_\gamma} J_{\text{inc}} \rho d \Delta\Omega_e \Delta\Omega_\gamma , \tag{4.1}$$

where J_{inc} is the average incident electron flux, ρ is the target density, d is the target thickness, and $\Delta\Omega_i$ is the solid angle of detection for particles of type i.

The e-γ coincidence cross sections are presented with superconducting accelerators of the near future in mind. In estimating the counting rates of the above cross section, an incident electron current of 100 μA for 200-MeV electrons is used. In all cases considered here the cross sections appear to be large enough to yield detectable counting rates. Remaining is the question of relative size of the background counting rate due to other processes.

As mentioned before, a main interfering process is elastic electron scattering from the nucleus plus emission of electron bremsstrahlung. An estimate of the size of the e-γ coincidence cross section for this process can be obtained by treating the nucleus as a point charge. In the soft photon limit the e-γ coincidence cross section is[12]

$$\frac{d^2\sigma}{d\Omega_e d\Omega_\gamma} = \left(\frac{d\sigma}{d\Omega_e}\right)_{\text{IN}} \frac{\alpha}{4\pi^2} \ln\frac{k_{\max}}{k_{\min}} \left[\frac{2(1-\cos\theta_e)}{(1-\hat{k}\cdot\vec{\beta}_f)(1-\hat{k}\cdot\vec{\beta}_i)} - \frac{m_e^2}{E_f^2(1-\hat{k}\cdot\vec{\beta}_f)^2} - \frac{m_e^2}{E_i^2(1-\hat{k}\cdot\vec{\beta}_i)^2}\right], \tag{4.2a}$$

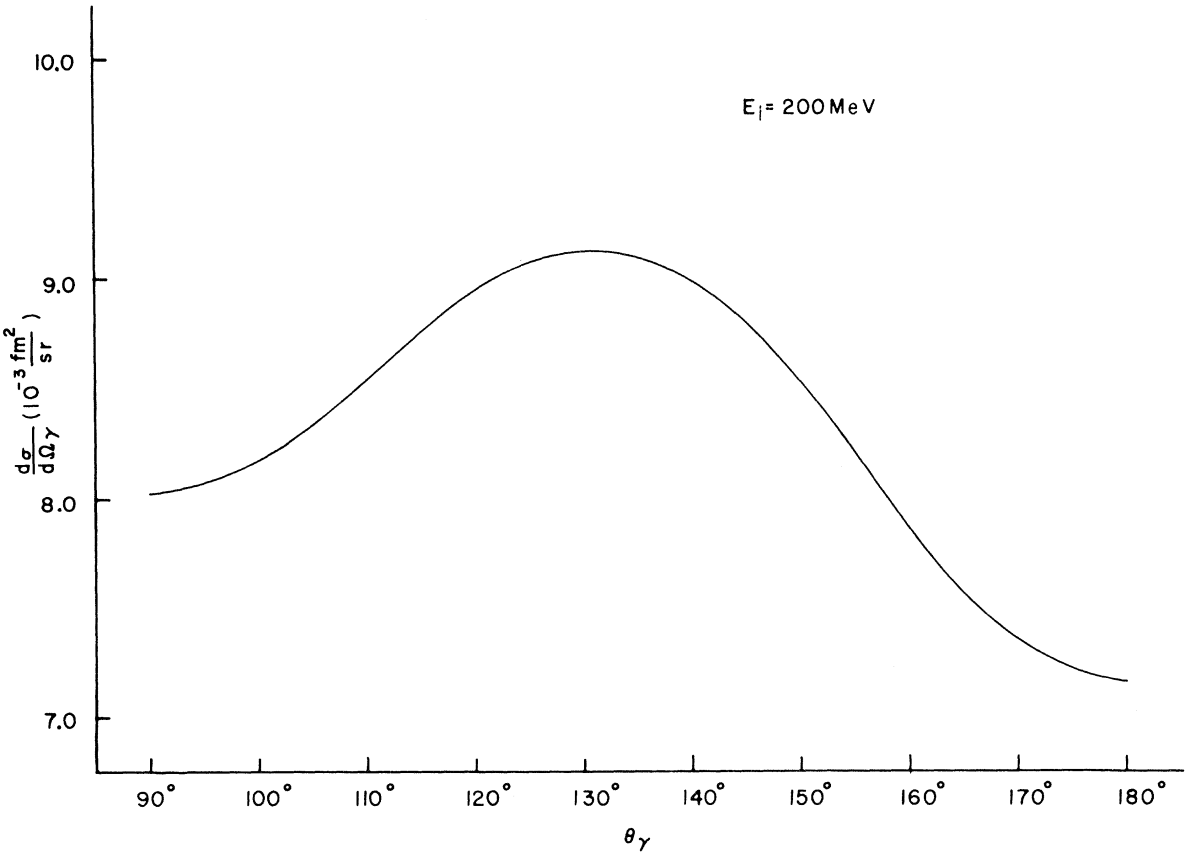

FIG. 11. γ-detection cross section for $_{73}Ta^{181}$ with the decay assumed to be a pure $E2$ transition.

where

$$\left(\frac{d\sigma}{d\Omega_e}\right)_{IN} = \frac{Z^2\alpha^2}{4p^2\beta^2\sin^4\frac{1}{2}\theta_e}(1-\beta^2\sin^2\tfrac{1}{2}\theta_e). \qquad (4.2b)$$

The electron scattering angle is θ_e, $\hat{k}$ is the unit vector in the direction of the photon, $\vec{\beta}_i$ and $\vec{\beta}_f$ are the velocity vectors for the initial and final electron. The cross section is for photons with energy in the range k_{min} to k_{max}. The e-γ cross section for $E_i = 200$ MeV, $\theta_e = 140$, $\phi_e = 0°$, $\theta_\gamma = 180°$, k_{min} to k_{max} taken to be 103 to 140 keV, and $Z = 73$ is

$$d^2\sigma/d\Omega_e d\Omega_\gamma \cong 9.65\times10^{-5}\,\mathrm{fm^2/sr^2}. \qquad (4.3)$$

This cross section can be compared to the e-γ coincidence cross section for the electron-excitation–$E2$-decay reaction with $_{73}Ta^{181}$. For the same kinematics as above the e-γ coincidence cross section is

$$d^2\sigma/d\Omega_e d\Omega_\gamma \cong 1.70\times10^{-2}\,\mathrm{fm^2/sr^2}. \qquad (4.4)$$

Thus, the interference from the electron bremsstrahlung is negligible for the proper choice of the kinematics.

Interference from cascade decays resulting from electron excitation of more energetic nuclear states must be investigated for each nucleus and depends on the electron energy resolution. Only more energetic states which lie within the electron energy resolution of the state to be investigated can result in cascade decays producing the γ rays sought. As mentioned before, these reactions are of higher order in α than the process considered here and can be expected to have smaller amplitudes by at least a factor of α.

On the basis of the results presented in Sec. III the e-γ coincidence cross section appears to provide a means for investigating low-lying nuclear states when superconducting accelerators become operational.

The γ-detection cross sections were calculated with present-day experimental capabilities in mind. The γ counting rate for photons produced by the electron-excitation–γ-decay reaction can be estimated using the relation

$$R_\gamma = (d\sigma/d\Omega_\gamma)J_{inc}\rho d\Delta\Omega_\gamma. \qquad (4.5)$$

The counting rates were estimated assuming an average electron current of 1 μA. Again the cross section appears to be large enough, provided the background counting rate for photons is not too

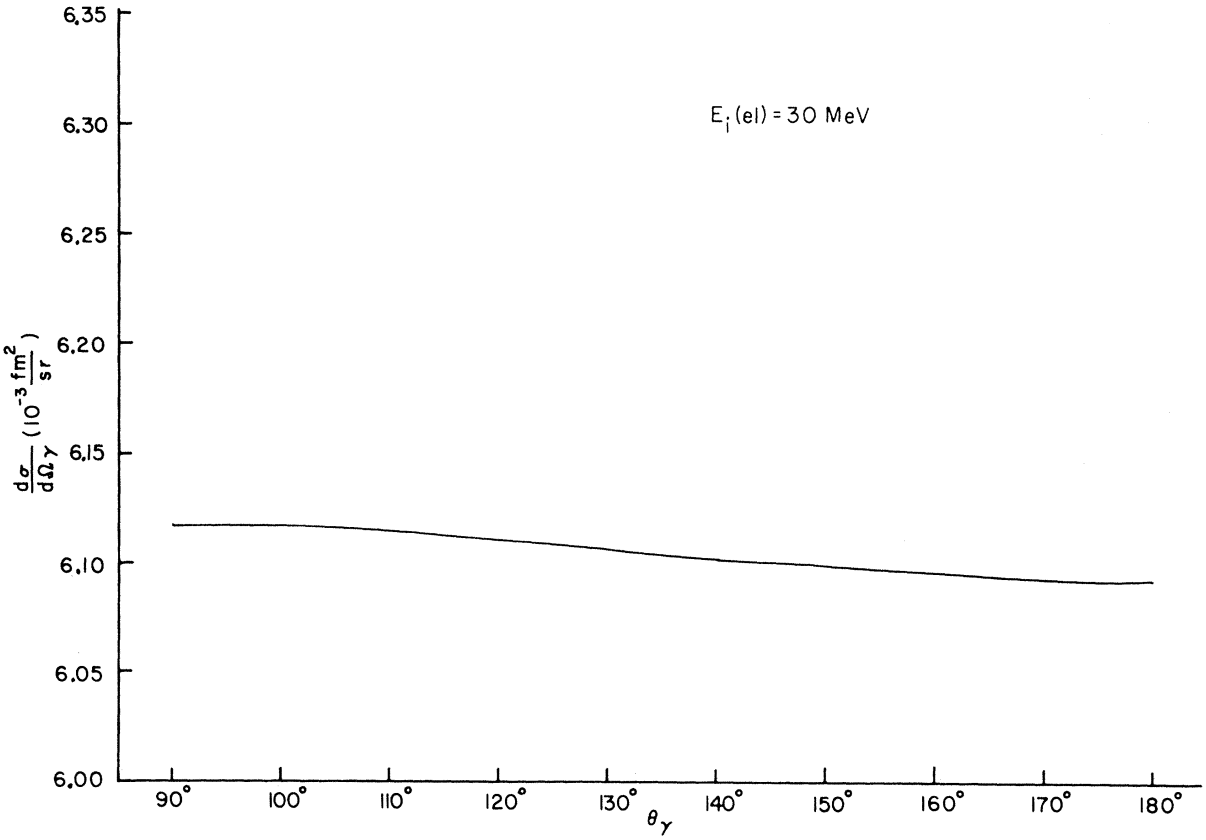

FIG. 12. γ-detection cross section for $_{73}Ta^{181}$ with the decay assumed to be a pure $M1$ transition.

large. The results for $E_i = 30$ MeV are particularly encouraging in view of the large electron current available at lower energies.

The interference from elastic electron scattering plus bremsstrahlung can be minimized by detecting the photons at large angles to the incident electron beam. The e-γ cross section is strongly peaked in the forward electron scattering direction. Thus the main contribution to the γ-detection cross section comes from the small-electron-angle e-γ cross section. As seen above, the bremsstrahlung interference is small for small electron scattering angles and large photon angles relative to the incident beam. As before, the interference from cascade decays resulting from excitation of higher-energy nuclear states is of higher order in α.

Thus the results for the γ-detection cross section also appear to be favorable for investigating low-lying states in heavy nuclei.

APPENDIX A.

The electron wave functions are solutions to the Dirac equation for an electron in a central potential due to the static Coulomb field of the nucleus. The Dirac equation can be written in the form[13]

$$H\psi = E\psi, \tag{A.1}$$

where

$$H = i\gamma_5\sigma_r\left(\frac{\partial}{\partial r} + \frac{1}{r} - \frac{\beta}{r}K\right) + V(r) + m\beta.$$

Solutions to this equation, which are eigenstates of the operators $\vec{j}^2$, j_z, and $K = \beta(\vec{\sigma}\cdot\vec{l} - 1)$, can be written as

$$\psi_\kappa^\mu = \begin{pmatrix} g_\kappa(r)\, X_\kappa^\mu \\ if_\kappa(r)\, X_{-\kappa}^\mu \end{pmatrix}, \tag{A.2}$$

where

$$K\psi_\kappa^\mu = \kappa\psi_\kappa^\mu,\ j = |\kappa| - \tfrac{1}{2},\ \text{and}\ j_z = \mu.$$

The spin and angular dependence of ψ is contained in X_κ^μ which is given by

$$X_\kappa^\mu = \sum_\tau C^l_{\mu-\tau\ \tau\ \mu}{}^{1/2\ j}\, Y_l^{\mu-\tau}(\hat{r})\, X_{1/2}^\tau, \tag{A.3}$$

where $l = \kappa$ for $\kappa > 0$, and $l = -\kappa - 1$ for $\kappa < 0$.

The radial parts of the wave function are solutions to the coupled differential equations

$$\frac{df_\kappa(r)}{dr} = \frac{\kappa - 1}{r} f_\kappa(r) - [E - m - V(r)]g_\kappa(r), \tag{A.4a}$$

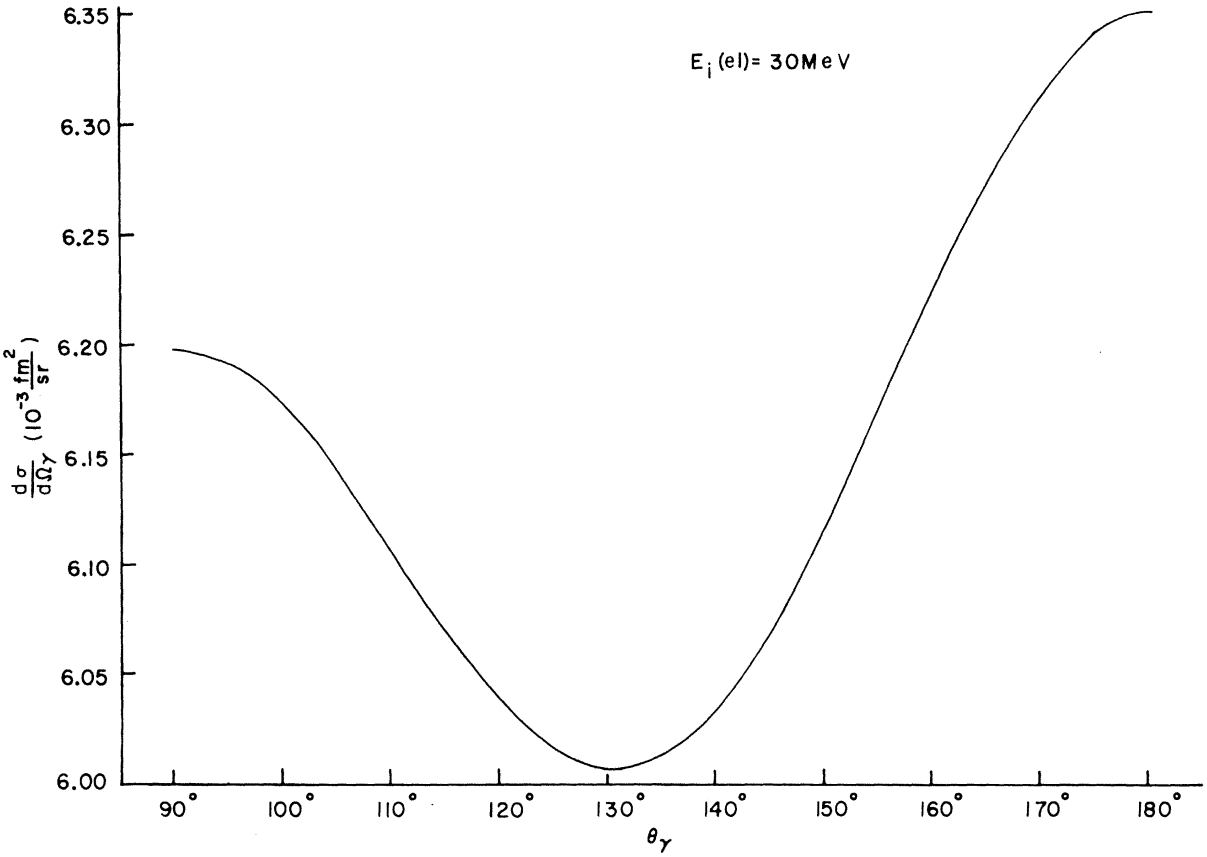

FIG. 13. γ-detection cross section for $_{73}Ta^{181}$ with the decay assumed to be a pure $E2$ transition.

$$\frac{dg_\kappa(r)}{dr} = [E+m-V(r)]f_\kappa(r) - \frac{\kappa+1}{r} g_\kappa(r), \quad \text{(A.4b)}$$

which have the asymptotic form

$$f_\kappa(r) \sim \left(\frac{E-m}{E+m}\right)^{1/2} \frac{1}{pr} \sin(pr+\delta_\kappa), \quad \text{(A.5a)}$$

$$g_\kappa(r) \sim \frac{1}{pr} \cos(pr+\delta_\kappa). \quad \text{(A.5b)}$$

Using these solutions, a partial wave expansion for an incident plane wave with momentum p plus outgoing spherical waves can be formed. For a polarized beam with spin projection m ($=\pm\frac{1}{2}$) on the z axis, the partial wave expansion is

$$\psi^m = 4\pi \left(\frac{E+m}{2E}\right)^{1/2} \sum_\mu e^{i\bar{\delta}_\kappa} i^l C^l_{\mu-m\, m\, \mu}{}^{1/2\, j} Y^{\mu-m*}_l(\hat{p}) \psi^\mu_\kappa . \quad \text{(A.6)}$$

The phase $\bar{\delta}_\kappa$ is given by

$$\bar{\delta}_\kappa = \delta_\kappa - y \ln 2pr + \tfrac{1}{2}(l+1)\pi, \quad \text{(A.7)}$$

where $y = \alpha ZE/p$.

---

*Work supported in part by the U. S. Atomic Energy Commission.

[1]W. C. Barber, Ann. Rev. Nucl. Sci. 21, 1 (1962).
[2]T. deForest, Jr., and J. D. Walecka, Advan. Phys. 15, 1 (1966).
[3]H. A. Schwettman, private communication.
[4]D. F. Hubbard and M. E. Rose, Nucl. Phys. 84, 377 (1966).
[5]H. L. Acker and M. E. Rose, Ann. Phys. (N.Y.) 44, 336 (1967).
[6]D. Drechsel and H. Überall, Phys. Rev. 181, 1383 (1969).
[7]T. A. Griffy, D. S. Onley, J. T. Reynolds, and L. C. Biedenharn, Phys. Rev. 128, 833 (1962).
[8]K. Alder, A. Bohr, T. Huus, B. Mottelson, and A. Winther, Rev. Mod. Phys. 28, 432 (1956).
[9]We obtain a slightly different result from that given in Ref. 8. In a similar equation on p. 441 of Ref. 8, Alder *et al.* have $(-)^\mu$ where we have $(-)^{\mu\kappa}$.
[10]P. H. Pratt, J. D. Walecka, and T. A. Griffy, Nucl. Phys. 64, 677 (1965).
[11]J. F. Ziegler, Yale University Report No. Yale-2726E-49, 1967 (unpublished).
[12]J. D. Bjorken and S. D. Drell, *Relativistic Quantum Mechanics* (McGraw-Hill Book Company, Inc., New York, 1964).
[13]M. E. Rose, *Relativistic Electron Theory* (John Wiley & Sons, Inc., New York, 1961).